

## Supporting information

# Step-Controllable Electric-Field-Assisted Nanoimprint Lithography for Uneven Large-Area Substrates

*Chunhui Wang,<sup>†§</sup> Jinyou Shao,<sup>†\*</sup> Hongmiao Tian,<sup>†</sup> Xiangming Li,<sup>†</sup> Yucheng Ding,<sup>†</sup> and Ben Q. Li<sup>‡</sup>*

<sup>†</sup>Micro- and Nano-technology Research Center, State Key Laboratory for Manufacturing Systems Engineering, Xi'an Jiaotong University, Xi'an, Shaanxi 710049, China

<sup>§</sup>Shaanxi Province Key Laboratory of Thin Film Technology and Optical Test, Xi'an Technological University, Xi'an, Shaanxi 710032, China

<sup>‡</sup>Department of Mechanical Engineering, College of Engineering and Computer Science, University of Michigan - Dearborn, Dearborn, Michigan 48128, USA

\*Corresponding authors: jyshao@mail.xjtu.edu.cn(Jinyou Shao);

**Corresponding Author:** Jinyou Shao, jyshao@mail.xjtu.edu.cn;

## 1. Electrostatic attraction and electrocapillary driven joint filling of template

Besides propagating the contact front between the template and substrate, an applied electric field is also helpful to operate the liquid resist fill the template. Figure S1 shows the simulation of the progressive evolution of liquid resist at the cross-section of nanohole based on the phase-field formulation<sup>32</sup> of liquid dielectrophoresis, whose depth is 500 nm and diameter is 300 nm while the other parameters are the same as the above experiment when the applied voltage is 500 V. In the numerical simulation, it is assumed that the air/polymer interface is planar at the initial contact of the template with the resist as shown in Figure S1 (a i). Once dc voltage is applied, the top resist surface moved gradually upward with a spatially non-uniform velocity. Because the template is movable relative to the substrate, two forces will drive the polymer flow: the electrostatic-attraction  $P$  between the template and the substrate as shown in eq 3, and volumetric dielectrophoresis–electrocapillary force  $F_{dep}$  acting on the resist surface, which is due to the Maxwell stress given in

$$F_{dep} = -\frac{1}{2}E^2\nabla\epsilon_{rf} \quad (S1)$$

where the resist and air are assumed to be dielectric media with no volumetric free charge density, and  $\epsilon_{rf}$  is the permittivity of the fluid, comprising air and resist in the two-phase filled formulation. Under the combination of these two driving pressures, the resist surface rises to the highest centrally in the cavity, as shown in Figure S1 (a ii). This causes the resist to reach the center of the bottom of the cavity first, compressing the trapped air towards the corner of the cavity, as shown in Figure S1 (a iii). The final shape of the resist is determined by a static equilibrium between the hydraulic pressure of trapped air and electrostatic pressure.

Figure S1 (b) shows the rising height of the central resist surface with respect to the time (the electrically actuated time scaled to the time taken for the central resist surface to reach the

bottom of the cavity under the combined effect) simulated for  $P$ , and  $F_{dep}$  is effective alone separately and in combination. From the lines, the combination of  $P$  and  $F_{dep}$  can be determined as the driven force to actuate the hydrodynamic behaviors with a faster filling speed, but whichever force drives singly is slow. Therefore, either attraction  $P$  or electrocapillary  $F_{dep}$  play an important role in actuating the resist flow to this nanohole cavity.

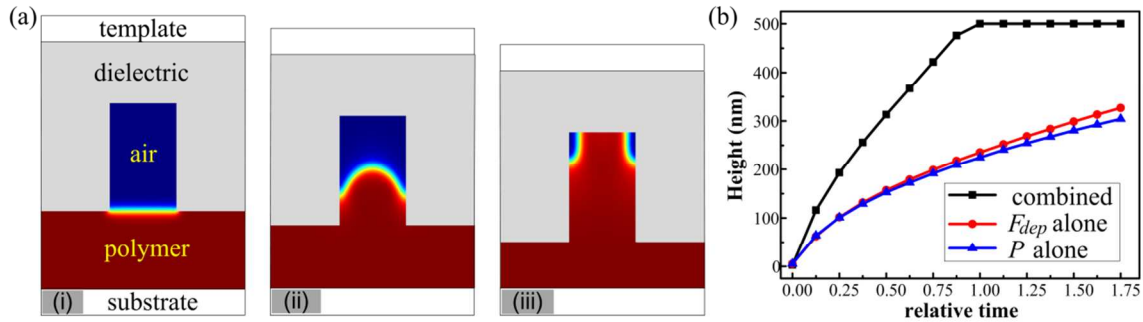


**Figure S1.** (a) Progressive evolution of resist at an applied voltage of 500 V to a nanohole of depth 500 nm and diameter 300 nm. (b) Rising height of the central resist surface with respect to the time scale under different driving pressures (dielectrophoresis–electrocapillary  $F_{dep}$  effective alone, electrostatic-attraction  $P$  effective alone, and their combination effective).

## 2. Voltage effect of electric field assisted contact progress

To analyze the effective voltage range, the initial mode about contact progress between flexible template and liquid resist under a certain voltage is established as shown in Figure S2. The progress of contact front propagating under an external electric field can be depicted by elastic theory of plate and electrohydrodynamic theory as eq 1 ~ 4. When applying one voltage on the electric pair, contact front is driven by electrostatic-attraction pressure  $P$  and electrostatic-liquid-bridging force  $F_{el}$  two parts at the same time. In order to simply the modeling process,

moment equilibrium about the plate is established, which the resultant moment of these two forces are used to consider as the drive, and the deformation of the plate is the obstruction.

About the drive moment,

$$M_P = \int_{x_0}^L P(L-x)dx = \frac{\varepsilon_r^2 \varepsilon_0}{2} \left(\frac{UL}{H}\right)^2 \left(\frac{L}{x_0} + \ln x_0 - \ln L - 1\right) \quad (\text{S2})$$

$$M_{el} = aF_{el}(L-x_0) = 8a\gamma\cos\theta_U(L-x_0)^2/H \quad (\text{S3})$$

$$M_E = M_P + M_l \quad (\text{S4})$$

where  $x_0$  the contact position,  $H$  the height of the spacer and  $L$  the total length of the substrate,  $a$  the width of the flexible template,  $M_P$  and  $M_{el}$  respectively are the drive moment of  $P$  and  $F_{el}$ , and  $M_E$  the resultant moment formed by applied electric field.

On the other hand, the resisting moment of resulting plate deformation can be calculated according to elastic theory when supposing there is no any load on the plate by solving the governing equation

$$w'''' = 0 \quad (\text{S5})$$

with the following four boundary conditions:

$$\begin{cases} w_{x_0} = 0 \\ w'_{x_0} = 0 \\ w_L = H \\ w''_L = 0 \end{cases} \quad (\text{S6})$$

then the resisting moment can be described as

$$M_0 = w''_L EI \quad (\text{S7})$$

When  $M_E = M_0$ , the biggest contact length  $L_c$  under one voltage can be calculated. Scanning the applied voltage, we can learn the voltage range and the saturation value as shown in Figure 2(b).

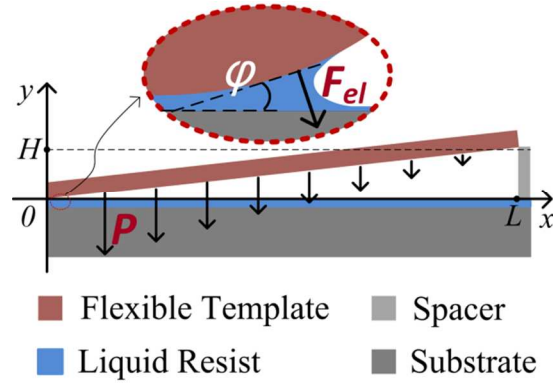


**Figure S2.** The initial contact model between the flexible template and the substrate coated with liquid resist.

### 3. PhC nanostructures imprint by natural capillary force

Figure S3 shows the PhC nanostructures image on 4" uneven GaN epi-wafer by step-controllable e-NIL when  $U = 0$  and the other conditions is the same to the experiment process in Figure 6. Figure S3(a) shows the obvious local structuring failure area that is much bigger than a single LED chip (generally is  $\sim 100 \mu\text{m}$ ), which is unacceptable in HB-LED fabrication process. The sample implemented here is from the same batch with that shows in Figure 6, both their surface profile bow measurement results ( $\sim 150 \mu\text{m}$  measured by Taylor Hobson PGI 3D) is shown in Figure S3(b). Though in some local position that the interference color was uniform from the photo in Figure S3(a), the magnifying moiré fringes as show in Figure S3(c) exposes the defect, and Figure S3(d), is the magnified trapping air defect area.

The main reason for the failure is the limited drive force, namely the only liquid-bridging force  $F_{LS}$ , is not sufficient to deform the flexible template that with the higher liquid resist contact angle. This provides the effective proof to the proposed step-controllable e-NIL method from the other side.

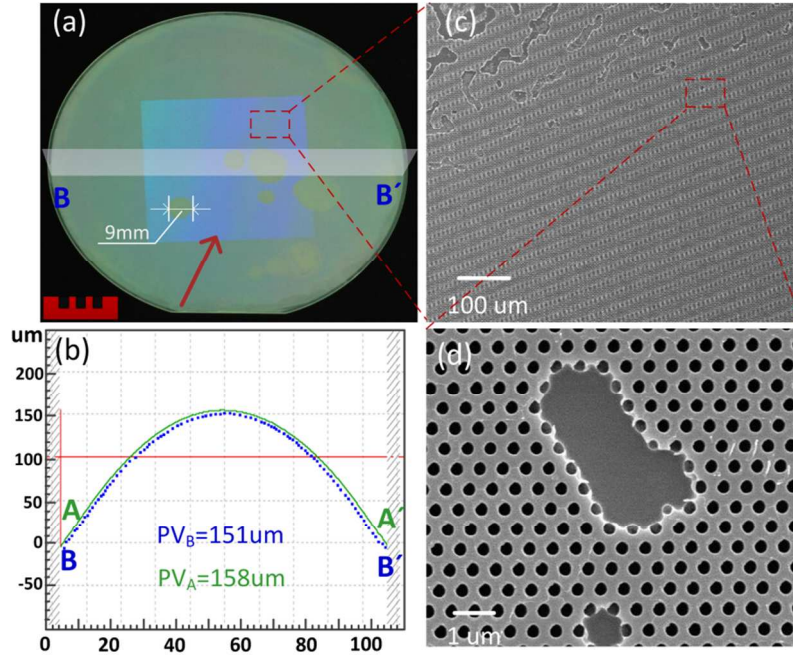


**Figure S3.** PhC fabrication on 4'' GaN epi-wafer without electric field. (a) Photo of GaN epi-wafer with obvious local structuring failure area, the red arrow is the spread direction of contact front. (b) Epi-wafer surface profile measurement result, nearly the same to the previous wafer, A, A' and B, B' are the testing endpoints in different samples; (c) Confusion in SEM *moiré*. (f) A trapping air defect area.